PHYSICAL REVIEW B **81**, 245214 (2010)

Thermal expansivity of $Ge_{1-y}Sn_y$ alloys

R. Roucka,[1] Y.-Y. Fang,[1] J. Kouvetakis,[1] A. V. G. Chizmeshya,[1] and J. Menéndez[2]
[1]*Department of Chemistry and Biochemistry, Arizona State University, Tempe, Arizona 85287-1604, USA*
[2]*Department of Physics, Arizona State University, Tempe, Arizona 85287-1504, USA*
(Received 19 February 2010; revised manuscript received 1 May 2010; published 29 June 2010)

The temperature dependence of the lattice parameter of $Ge_{1-y}Sn_y$ alloys deposited on Si substrates has been determined from an analysis of their x-ray reciprocal-space maps. It is found that over the range $0<y<0.03$ the alloy thermal expansivity increases by up to 20% as a function of y. This implies a strong deviation from a linear interpolation between the end compounds since the thermal expansivities of pure Ge and α-Sn are nearly the same. Alternative interpolation formulas based on a Debye model and a mixed Debye-Einstein model of the phonon structure are tested and it is found that they also fail to explain the observed increase in thermal expansivity.

DOI: 10.1103/PhysRevB.81.245214 PACS number(s): 65.40.De, 81.05.Bx, 81.05.Cy

I. INTRODUCTION

The thermodynamic properties of group-IV materials—measured more than half a century ago—still represent an important test bed for theoretical methods, in particular, modern *ab initio* approaches.[1–6] One such property, the thermal expansivity, has acquired particular relevance over the past decade in the context of epitaxial growth of materials. The difference in thermal expansivity (commonly referred to as thermal-expansion coefficient) between the substrate and the grown film generates stresses that affect the film's electronic and optical properties. Such expansivity mismatches offer some intriguing engineering opportunities. A recent example is the use of the much larger thermal expansivity of Ge relative to Si (5.8×10^{-6} versus 2.56×10^{-6} K^{-1} at room temperature) to generate a tensile strain in Ge films that grow relaxed on Si at high temperatures. This tensile strain, which develops upon cooling to room temperature, lowers the band gap and allows Ge-based detectors to offer a better coverage of the so-called L window for telecommunications.[7]

The phonon-dispersion curves of the group-IV materials Si, Ge, and α-Sn (and, to a lesser extent, diamond) scale very well with the so-called ionic plasma frequency $\Omega \propto M^{-1/2}V_c^{-1/2}$, where M is the atomic mass and V_c the volume of the unit cell.[8] In particular, the corresponding Debye temperatures $\Theta_D(\mathrm{Si})=645$ K (Ref. 9), $\Theta_D(\mathrm{Ge})=347$ K (Refs. 9 and 10), and $\Theta_D(\alpha\text{-Sn})=212$ K (Ref. 11) follow the same scaling, suggesting that the thermal expansivities of the three materials should be similarly related. Using a Debye model for the phonons, and assuming a common Grüneisen parameter $\gamma=0.5$, the linear thermal expansivity at the Debye temperature is given by $\alpha(\Theta_D)=3.81k_B/(a^3B)$, where B is the bulk modulus. Cohen[12] has pointed out that the bulk modulus scales as $a^{-7/2}$, so that we might expect $\alpha(\Theta_D)\propto a^{1/2}$. According to this, the linear thermal expansivities of Si, Ge, and α-Sn at the Debye temperature should be in a 1:1.02:1.09 ratio, but the experimental ratios are 1:1.6:1.5 (Refs. 11 and 13–16). There are two reasons for this poor agreement with experiment. First, as already noted by Cohen,[12] the Ge bulk modulus is anomalous in terms of his proposed scaling, its experimental value being below the predicted one. This enhances the Ge thermal expansivity. Second, the average Grüneisen parameters at the corresponding Debye temperatures are $\gamma_{\mathrm{Si}}=0.56$, $\gamma_{\mathrm{Ge}}=0.78$, and $\gamma_{\mathrm{Sn}}=0.79$.[3,5,11] This enhances the Ge and α-Sn thermal expansivities relative to that of Si. It might come as a surprise that the α-Sn Grüneisen parameter turns out be comparable to that of Ge since we might expect α-Sn to be more anharmonic than Ge or Si. In fact, if we consider the width/frequency ratio of the Raman peaks for isotopically pure Si (Ref. 17), Ge (Ref. 18), α-Sn (Ref. 19), we find values of 0.2% for Si and Ge, and 0.3% for α-Sn, confirming the higher anharmonicity of the α-Sn Raman mode. The average Grüneisen parameter, however, is a weighted average of the Grüneisen parameters for all individual phonons, some of which are negative. Thus an increase in anharmonicity which disproportionally enhances the absolute value of the negative Grüneisen parameters might lead to a reduction in the average value.

In view of the difficulty in understanding the chemical trends in the linear expansivity of elemental group-IV materials, predicting the compositional dependence of this property in group-IV alloys appears to be a formidable task. From an experimental perspective, very few detailed studies have been published. In the case of $Si_{1-x}Ge_x$ alloys, a monotonic decrease from pure Ge to pure Si has been determined, with a clear change in slope at $x\sim0.85$ (Ref. 20). This corresponds to the composition at which the lineup of the conduction-band minima changes from Si-like to Ge-like. There is no obvious way to relate the thermal expansivity to the details of the conduction-band structure, and this puzzling finding remains for now an accidental coincidence.

In this paper, we report a study of the thermal expansivity of $Ge_{1-y}Sn_y$ alloys. At room temperature, the thermal expansivities of Ge and α-Sn are nearly the same, and one might expect the alloy thermal expansivity to become independent of the Sn-concentration y. This would have important implications for device designs based on $Ge_{1-y}Sn_y$ and $Ge_{1-x-y}Si_xSn_y$ active layers. However, we find a strong increase in the thermal expansivity as a function of y for low Sn concentrations. We show that this anomalous result cannot be reconciled with any simple theory of the compositional dependence of the linear expansivity. We speculate that it may be related to a softening of the alloy bulk modulus or to a strong compositional dependence of the Grüneisen parameters.

II. EXPERIMENT

A. Sample growth and characterization

GeSn films with thickness up to 1 μm are grown on Si substrates with a nominal size of 3″ in diameter via reactions of SnD_4 with Ge_2H_6, as described elsewhere.[21] The samples are characterized by Rutherford backscattering (RBS), atomic force microscopy, high-resolution transmission electron microscopy (HRTEM), and high-resolution x-ray diffraction (XRD). The ratio of aligned versus random peak heights in RBS spectra (χ_{min}), which measures the degree of crystallinity, decreases from 10% at the interface to 5% at the surface, indicating a reduction in dislocation density across the thickness of the film. The 5% value approaches the practical limit of ~3% for a perfect Si crystal, suggesting that most of the defects accommodating the lattice mismatch between film and substrate are confined at the interface. This is consistent with HRTEM pictures showing essentially defect-free films. The concentration of residual threading defects and the mosaic spread of the crystal are improved by performing for all samples three rapid-thermal annealing (RTA) cycles of 10 s each at 650 °C. This postgrowth processing reduces the full width at half maximum of the (004) rocking curve.

B. Temperature dependence of the lattice constant

The temperature dependence of the lattice constant was measured using a PANalytical diffractometer equipped with an Anton Paar high-temperature stage. The heating was conducted under inert atmosphere conditions in a dynamic flow of ultrahigh-purity nitrogen at a 4 psi overpressure to avoid oxidation and degradation of the films by the ambient (H_2O and O_2). At each temperature the sample was realigned using the Si (224) reflection to correct for any drift associated with the hot stage expansion. The samples were heated to a series of temperatures between 30 and 600 °C. The unit-cell parameters of all GeSn films and a Ge film on Si were determined from measurements of the (004) $2\theta/\omega$ peaks and reciprocal-space maps (RSMs) of the (224) reflection. We used for all of our thermal expansivity studies samples that had undergone the RTA treatment described above. Figure 1 shows the room-temperature (224) RSM plot for a 1000-nm-thick, $Ge_{0.98}Sn_{0.02}$ sample indicating that the material is largely relaxed, as evidenced by the passage of the relaxation line through the center of the peak.

In spite of the small residual strain, a strain correction is necessary to obtain the film's thermal expansivity due to the expansivity mismatch between film and substrate. Assuming that the strain has tetragonal symmetry, the relaxed lattice constant for the film material at each temperature is obtained from

$$a = \frac{a_\perp + \frac{2C_{12}}{C_{11}} a_\parallel}{1 + \frac{2C_{12}}{C_{11}}}, \tag{1}$$

where $a_\parallel$ is the tetragonal lattice constant in the growth plane and $a_\perp$ the lattice constant perpendicular to the growth plane.

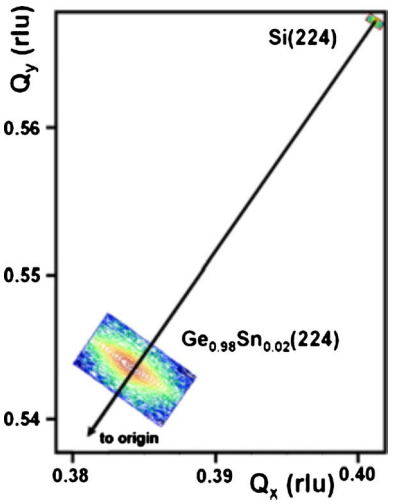

FIG. 1. (Color online) High-temperature XRD plot recorded at 30 °C showing the (224) reciprocal-space maps of a fully relaxed $Ge_{0.98}Sn_{0.02}$ film and the corresponding Si substrate.

According to Eq. (1) the determination of the relaxed lattice parameter requires a prior knowledge of the alloy elastic moduli ratio C_{12}/C_{11} as a function of composition and temperature. However, since in the limit $a_\parallel \to a_\perp$, Eq. (1) becomes independent of C_{12}/C_{11}, the elastic moduli ratio need not be known with very high accuracy whenever the difference between $a_\parallel$ and $a_\perp$ is small. This is the case in our experiments due to the low strain level, as shown in Fig. 1. Thus we simply use C_{12}/C_{11} values for pure Ge in Eq. (1). We believe this is an excellent approximation for the alloy because of the above-mentioned scaling of phonon-dispersion curves in Si, Ge, and α-Sn (Ref. 8), from which *ratios* of elastic constants, such as C_{12}/C_{11}, are expected to have very similar values. This is experimentally confirmed[22] in the case of Si(C_{12}/C_{11}=0.386) and Ge(C_{12}/C_{11}=0.375) We thus expect the compositional dependence of the C_{12}/C_{11} ratio in group-IV alloys to be weak. Moreover, the temperature dependence of the C_{12}/C_{11} ratio is much weaker than the temperature dependence of the individual elastic moduli, and could be neglected without a significant impact on the calculated relaxed parameters. For completeness, however, we have fit the Ge C_{12}/C_{11} ratio from McSkimin,[23] obtained in the 70–300 K range, with a linear function of temperature, and we extrapolate these results to the temperatures of interest in this study. Thus the final expression we use is

$$\frac{C_{12}}{C_{11}} = 0.37492 - 3.7 \times 10^{-6} T, \tag{2}$$

where the temperature T is in Celsius. It is interesting to note in this context that Burenkov *et al.* (Ref. 24) have measured the elastic moduli of Ge within the 0–800 °C range, which overlaps of with our measurements. Their data can be fit with an expression of the form $C_{12}/C_{11}=0.338-4.5\times10^{-6}T$. We prefer the highly accurate McSkimin data, however, because the Burenkov *et al.* C_{12}/C_{11} ratios have much larger fluctuations. Moreover, Brillouin scattering experiments are in much better agreement with the McSkimin elastic

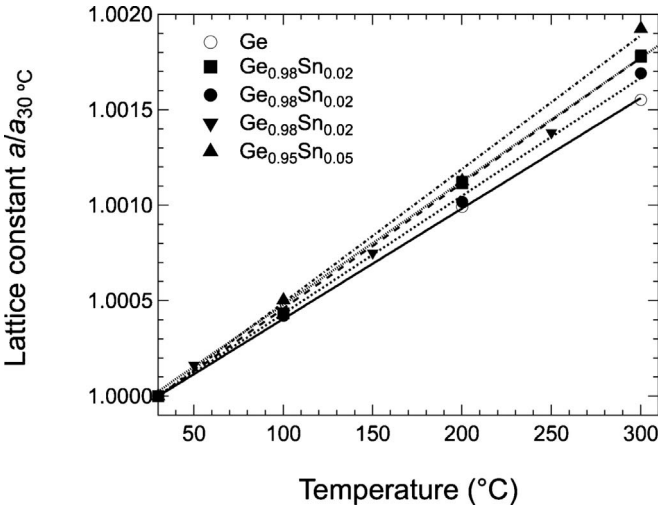

FIG. 2. Relaxed lattice parameter of $Ge_{1-y}Sn_y$ alloys as a function of temperature. The data is normalized to the relaxed lattice parameter at 30 °C. The slope of a linear fit to the data gives the average thermal expansivity within the temperature range of the fit. The compositions are obtained from fits of RBS spectra.

constants.[25] Nevertheless, we emphasize that the choice of elastic moduli sets is not critical for our purposes. The final values of the thermal expansivity, defined as

$$\alpha(T) = \frac{1}{a(T)}\frac{da(T)}{dT} \tag{3}$$

differ by about 1×10^{-7} °C^{-1} using the two sets of elastic moduli ratios. As we will see below, this is comparable to the uncertainty arising from other sources of accidental errors.

As a first application of our procedure to obtain the relaxed lattice constants, we compared films before and after RTA processing. We noticed that in all cases there is a change in the state of strain in the film, from slightly compressive after growth to slightly tensile after RTA. However, the *relaxed* lattice constant of films before and after RTA is the same within experimental error, confirming that thermal cycling does not cause irreversible changes that might introduce systematic errors in the thermal expansion measurements.

The most accurate approach to determine $\alpha(T)$ from Eq. (3) is to fit the experimental $a(T)$ values with a polynomial in T, from which the derivative da/dT can be trivially evaluated. The linear term in the polynomial fit is dominant in the temperature range of interest, to the extent that no deviation from linearity can be seen, within experimental error, between room temperature and 400 °C. Small quadratic terms become noticeable when including data up to 600 °C. However, since the accurate determination of these terms requires cycling the temperature several times to completely rule out any spurious contribution from Sn loss or film-substrate intermixing at high temperatures, we simply limit ourselves to the linear regime $T<400$ °C. This temperature is much lower than the RTA temperature so that systematic errors due to thermal cycling are minimized. Under these assumptions we obtain for the linear regime the approximate expression,

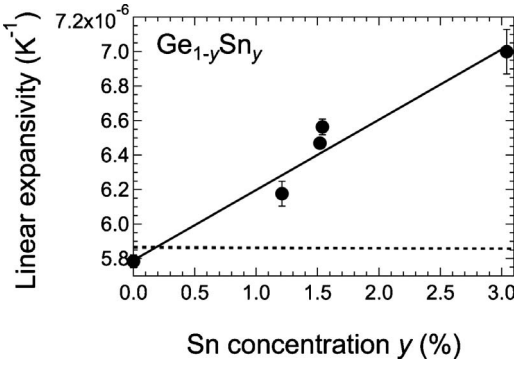

FIG. 3. Compositional dependence of the linear expansivity in $Ge_{1-y}Sn_y$ alloys. Circles represent experimental values extracted from linear fits of the data in Fig. 2. The error bars correspond to the errors in those fits. The solid line represents a linear fit of the expansivity as a function of composition. The dashed line is a theoretical prediction based on the two models discussed in Sec. III, which are undistinguishable over this narrow compositional range.

$$\frac{1}{a_0}\frac{da(T)}{dT} = \alpha, \tag{4}$$

where a_0 is taken as the lattice parameter at $T=30$ °C. In Fig. 2 we plot $a(T)/a_0$ over the 30–300 °C range.

According to Eq. (4), the slope of these lines gives directly the average thermal expansivity between 30–300 °C. This value is plotted in Fig. 3 as a function of the alloy composition. For this we derive more precise values of the composition from our measured lattice parameters at room temperature and the published compositional dependence of the lattice constant in $Ge_{1-y}Sn_y$ alloys.[26] This method is far more sensitive to small compositional changes than the fits to the RBS spectra used to obtain the nominal Sn concentrations in Fig. 2. We see a large increase in thermal expansivity in the alloys.

III. DISCUSSION

The linear thermal expansivity is given by[27]

$$\alpha(T) = \frac{1}{3B}\sum_{n,\boldsymbol{q}} \gamma_n(\boldsymbol{q})c_{n\boldsymbol{q}}, \tag{5}$$

where B is the bulk modulus, $\gamma_{n\boldsymbol{q}}$ the Grüneisen parameter of the vibrational mode of wave vector $\boldsymbol{q}$ and branch index n, and $c_{n\boldsymbol{q}}$ is this mode's contribution to the specific heat. If we replace the mode-dependent Grüneisen parameters by an average, mode-independent value, and assume a Debye model for the phonon-dispersion curves, the thermal expansivity for diamond-structure materials becomes

$$\alpha(T) = \frac{24k_B\gamma_D}{a^3B}\left(\frac{T}{\Theta_D}\right)^3 I_D(\Theta_D/T), \tag{6}$$

where k_B is Boltzmann's constant, a the cubic lattice parameter, and the Debye integral I_D is given by

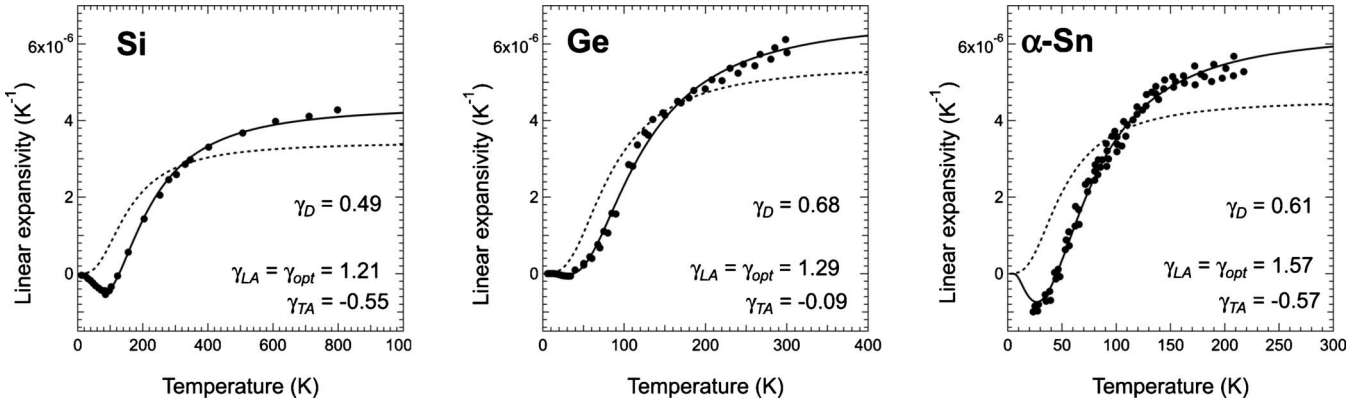

FIG. 4. Circles represent the experimental linear thermal expansivity for Si, Ge, and α-Sn. The data were taken from Ref. 13 (Si), Refs. 14, 15, and 29 (Ge), and Ref. 16 (Sn). The dashed lines represent fits with Eq. (6). The adjusted values of γ_D for each material are indicated in the three panels. The solid line is a fit with Eq. (8). The corresponding adjustable parameters, γ_{TA} and γ_{opt}, are also indicated in the three panels.

$$I_D(x_D) = \int_0^{x_D} \frac{x^4 e^x dx}{(e^x - 1)^2} = 24 \sum_{m=0}^{\infty} \left\{ 1 - \exp[-x_D(m+1)] \times \left(\sum_{k=0}^{4} \frac{[x_D(m+1)]^k}{k!} \right) \right\} \Big/ (m+1)^4. \quad (7)$$

The series expansion of the integral, due to Mamedov *et al.*,[28] is convenient for numerical fits with Eq. (6).

In Fig. 4 we show fits of the experimental thermal expansivities of Si, Ge, and α-Sn using Eq. (6). The agreement with experiment is not very good, but since Eq. (6) represents the simplest possible model of the thermal expansivity, it is instructive to attempt a prediction of the compositional dependence of the thermal expansivity based on this approach. For this we use Vegard's law for the lattice parameter and we also interpolate linearly the bulk modulus, the Debye frequency, and the average Grüneisen parameter that appear in Eq. (6). In order to match as close as possible the experimental values at the two ends of the compositional ranges, we use γ_D=0.47 for Si, γ_D=0.78 for Ge, and γ_D=0.83 for α-Sn. The result is shown as a dashed line in Fig. 5 for the $Si_{1-x}Ge_x$ and $Ge_{1-y}Sn_y$ alloys and also in Fig. 3 for $Ge_{1-y}Sn_y$ over the narrower range of our experiments.

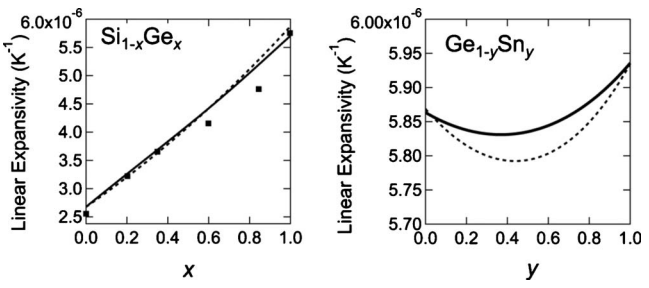

FIG. 5. Compositional dependence of the linear thermal expansivity at 300 K. Squares represent experimental data from Ref. 20. The dashed lines represents a prediction based on the Debye expansivity model in Eq. (6). The solid line is the corresponding calculation based on the mixed Debye-Einstein model of the expansivity in Eq. (8).

The predicted linear expansivity is almost linear over the entire compositional range for $Si_{1-x}Ge_x$ alloys and nearly constant for $Ge_{1-y}Sn_y$ alloys (notice the very different scale ranges in the two panels of Fig. 5) with a small negative bowing. The results for the $Ge_{1-y}Sn_y$ alloys are in sharp contrast with our experimental results. For $Si_{1-x}Ge_x$, the predicted compositional dependence of the expansivity does not show any significant change in slope at x=0.85, in contrast with the experimental reports.[20]

Since the Debye model is in rather poor agreement with the experimental thermal expansivity of elemental Si, Ge, and α-Sn, the predictions of the model for the compositional dependence of the thermal expansivity of group-IV alloys are unlikely to be reliable. Accordingly, we introduce a more sophisticated model that provides a very good fit of the thermal expansivity of Si, Ge, and α-Sn with a single additional parameter. The model considers separately the longitudinal-acoustic (LA), the transverse-acoustic (TA), and the optic (opt) modes. The LA modes are treated within a Debye model, whereas the TA and optic modes are described as two separate Einstein oscillators,

$$\alpha(T) = \frac{4k_B}{a^3 B_0} \left[\frac{2}{3} \gamma_{\mathrm{TA}} \left(\frac{\Theta_{\mathrm{TA}}}{T} \right)^2 \frac{e^{\Theta_{\mathrm{TA}}/T}}{(e^{\Theta_{\mathrm{TA}}/T} - 1)^2} + \gamma_{\mathrm{LA}} \left(\frac{T}{\Theta_{\mathrm{LA}}} \right)^3 \int_0^{\Theta_{\mathrm{LA}}/T} \frac{x^4 e^x dx}{(e^x - 1)^2} + \gamma_{\mathrm{opt}} \left(\frac{\Theta_{\mathrm{opt}}}{T} \right)^2 \frac{e^{\Theta_{\mathrm{opt}}/T}}{(e^{\Theta_{\mathrm{opt}}/T} - 1)^2} \right]. \quad (8)$$

It may seem counterintuitive to treat the TA modes in terms of an Einstein model, but the TA phonon-dispersion curves in tetrahedral semiconductors become very flat away from the Brillouin-zone center,[8] leading to sharp features in the phonon density of states. We choose the TA Einstein temperature as

$$\Theta_{\mathrm{TA}} = \hbar\, \omega_{\mathrm{TA}}(X)/k_B, \quad (9)$$

where $\omega_{\mathrm{TA}}(X)$ is frequency of the TA branch at the X point of the Brillouin zone, which is observed as a prominent

TABLE I. Fixed parameters used for the model fits to the experimental linear thermal expansivity of group-IV materials. The corresponding Grüneisen parameters are adjustable and their fit values are given in Fig. 4.

	Si	Ge	α-Sn
a (Å)	5.43086[a]	5.6568[a]	6.489[a]
B (GPa)	97.88[a]	75.8[a]	54.6[a]
Θ_D (K)	645[b]	347[b]	212[c]
Θ_{TA} (K)	217[d]	117[e]	60[f]
Θ_{LA} (K)	734[g]	411[g]	260[g]
Θ_{opt} (K)	673[h]	388[h]	255[h]

[a]Reference 32.
[b]Reference 9 at $T=0$ K.
[c]Reference 33 at $T=0$ K.
[d]From Eq. (9) with data from Ref. 30.
[e]From Eq. (9) with data from Ref. 31.
[f]From Eq. (9) with data from Ref. 34.
[g]From Eq. (11) with data from Ref. 32.
[h]From Eq. (10) with data from Ref. 32.

density-of-states cusp in second-order Raman-scattering experiments.[30,31] Similarly, the maximum of the optic-phonon density of states occurs at 90% of the zone-center optic-mode frequency, which can be determined by first-order Raman scattering. Accordingly, the optic Einstein temperature is chosen as

$$\Theta_{opt} = 0.9 \times \hbar\, \omega_R / k_B, \tag{10}$$

where ω_R is the first-order Raman frequency. Finally, the LA Debye temperature is given by

$$\Theta_{LA} = (\hbar c_{LA}/k_B)(2\pi/a)(3/\pi)^{1/3}, \tag{11}$$

where c_{LA} is the LA sound velocity. This velocity is direction dependent in diamond-structure semiconductors, but we make the isotropic approximation $2C_{44}=C_{11}-C_{12}$, so that all longitudinal sound velocities reduce to $c_{LA}=(C_{11}/\rho)^{1/2}$, where ρ is the density. The parameters used for the three materials are summarized in Table I.

With the Einstein and Debye temperatures so determined, the model of Eq. (8) contains three adjustable parameters, namely, the three Grüneisen parameters for the TA, LA, and optic modes. However, we find that the resulting fits are not very sensitive to the precise value of γ_{LA}, since the corresponding term accounts for only one of the six phonon branches, and its temperature dependence (particularly at high temperatures) is not dramatically different from that of the Einstein optic terms. Therefore, we set $\gamma_{LA}=\gamma_{opt}$, which is consistent with *ab initio* calculations.[3] The results of our two-parameter fits are shown in Fig. 4 as solid lines and we see that the agreement with experiment is excellent. Moreover, we notice that the above-mentioned relative Raman widths are approximately proportional to γ_{opt}^2, exactly as expected from anharmonicity theory,[35] since the Grüneisen parameters are proportional to third-order anharmonic matrix elements, whereas the Raman width is proportional to the square of such matrix elements.

The extension of our mixed Debye-Einstein model to alloy semiconductors must take into account the fact that the virtual-crystal approximation does not apply to optic vibrations. In the case of $Ge_{1-y}Sn_y$, for example, one must include three Einstein oscillators for Ge-Ge, Ge-Sn, and Sn-Sn vibrations, rather than a single Einstein oscillator with a frequency that changes continuously from pure Ge to pure α-Sn. As Sn is incorporated starting from pure Ge, the lower frequency of the Ge-Sn and Sn-Sn modes and the higher-optic Grüneisen parameter of α-Sn might lead to an increase in the predicted thermal expansivity relative to the prediction based on the Debye model. We calculate the alloy thermal expansivity using Eq. (8) with three optic Einstein oscillators, each with a relative weight given by $(1-y)^2$(Ge-Ge), $2y(1-y)$(Ge-Sn), and y^2(Sn-Sn). The Grüneisen parameter for the Ge-Ge and Sn-Sn modes are taken equal to those in pure Ge and α-Sn, and the average of these two values is taken as the Grüneisen parameter for the Ge-Sn mode. The Raman mode frequencies needed to calculate $\Theta_{opt}=0.9\times\hbar\,\omega_R/k_B$ are taken (in cm^{-1}) as[36] $\omega_{Ge\text{-}Ge}=300-75.4x$; $\omega_{Ge\text{-}Sn}=262.8-45.9x$, and $\omega_{Ge\text{-}Sn}=197$ cm^{-1}. All other quantities are linearly interpolated as in the case of the Debye model. Exactly the same approached is followed for Si_xGe_x alloys using mode frequencies from Ref. 37. The results appear as solid lines in Fig. 5. We find that the predicted thermal expansivities deviate very little from the predictions of the Debye model so that this more refined model also fails to explain the observed experimental data for both alloys.

We can only speculate as to the origin of the anomalous compositional dependence of the thermal expansivities. A first possibility might be a breakdown of our alloy phonon model due to the much larger atomic size differences between Ge and Sn compared with Si and Ge. Indeed, the Raman spectrum of $Ge_{1-y}Sn_y$ alloys has features that are not found in their $Si_{1-x}Ge_x$ counterparts.[38] However, these features have been explained in terms Raman selection rule relaxations rather than in terms of new vibrational modes, as would be necessary to explain the anomalous thermal effects reported here. Another possibility is a strongly nonlinear dependence of the bulk modulus for alloy compositions close to Ge, for which, as mentioned in Sec. I, the bulk modulus is lower than predicted from scaling laws.[12] However, experimental results[39] as well as *ab initio* calculations of alloy bulk moduli[26] do not seem to support large deviations from a linear interpolation. A third possibility is a strong compositional dependence of the Grüneisen parameters. A significant volume dependence of Grüneisen parameters has been calculated for Ge (Ref. 40) and Si (Ref. 41), and this might lead to a compositional dependence of the alloy Grüneisen parameters, since bond lengths in the alloy track the average lattice parameter.[42] Kagaya *et al.*[43] presented a model of the thermodynamic properties of $Si_{1-x}Ge_x$ alloys based on similar ideas. We notice in this context that Ge is anomalous not only from the point of view of its bulk modulus, as mentioned above, but also because the absolute value of its TA Grüneisen parameter is much smaller than that of Si or α-Sn (Fig. 4). We have used a linear interpolation of this parameter between the three elements, but if its value remains close

to that of pure Ge for Ge-rich $Si_{1-x}Ge_x$ and $Ge_{1-y}Sn_y$ alloys, this might explain the observed change in slope in the compositional dependence of the $Si_{1-x}Ge_x$ expansivity as well as the initial increase in expansivity in $Ge_{1-y}Sn_y$ alloys. Thus an examination of alloy Grüneisen parameters via large supercell *ab initio* calculations may be the key to explaining the puzzling results reported here.

ACKNOWLEDGMENTS

This work was supported by the U.S. Air Force under contract DOD AFOSR under Contract No. FA9550-06-01-0442 (MURI program), by the U.S. Department of Energy under Contract No. DE-FG36-08GO18003, and by the National Science Foundation under Grant No. DMR-0907600.

[1] J. Ihm and M. L. Cohen, Phys. Rev. B **23**, 1576 (1981).
[2] P. Pavone, K. Karch, O. Schütt, W. Windl, D. Strauch, P. Giannozzi, and S. Baroni, Phys. Rev. B **48**, 3156 (1993).
[3] S. Wei, C. Li, and M. Y. Chou, Phys. Rev. B **50**, 14587 (1994).
[4] A. Debernardi and M. Cardona, Phys. Rev. B **54**, 11305 (1996).
[5] Y. Ma and J. S. Tse, Solid State Commun. **143**, 161 (2007).
[6] A. Ward, D. A. Broido, D. A. Stewart, and G. Deinzer, Phys. Rev. B **80**, 125203 (2009).
[7] D. D. Cannon, J. Liu, Y. Ishikawa, K. Wada, D. T. Danielson, S. Jongthammanurak, J. Michel, and L. C. Kimerling, Appl. Phys. Lett. **84**, 906 (2004).
[8] W. Weber, Phys. Rev. B **15**, 4789 (1977).
[9] P. Flubacher, A. J. Leadbetter, and J. A. Morrison, Philos. Mag. **4**, 273 (1959).
[10] U. Piesbergen, Z. Naturforsch., A: Phys. Sci. **A18**, 141 (1963).
[11] R. W. Hill and D. H. Parkinson, Philos. Mag. **43**, 309 (1952).
[12] M. L. Cohen, Phys. Rev. B **32**, 7988 (1985).
[13] H. Ibach, Phys. Status Solidi B **33**, 257 (1969).
[14] D. F. Gibbons, Phys. Rev. **112**, 136 (1958).
[15] S. I. Novikova, Sov. Phys. Solid State **2**, 37 (1960).
[16] S. I. Novikova, Sov. Phys. Solid State **2**, 2087 (1961).
[17] F. Widulle, T. Ruf, A. Göbel, I. Silier, E. Schönherr, M. Cardona, J. Camacho, A. Cantarero, W. Kriegseis, and V. I. Ozhogin, Physica B **263-264**, 381 (1999).
[18] J. M. Zhang, M. Giehler, A. Göbel, T. Ruf, and M. Cardona, Phys. Rev. B **57**, 1348 (1998).
[19] D. T. Wang, A. Göbel, J. Zegenhagen, and M. Cardona, Phys. Rev. B **56**, 13167 (1997).
[20] V. V. Zhdanova, M. G. Kakna, and T. Z. Samadashvili, Izv. Akad. Nauk. SSSR, Neorg. Mater. **3**, 1263 (1967).
[21] M. Bauer, J. Taraci, J. Tolle, A. V. G. Chizmeshya, S. Zollner, D. J. Smith, J. Menendez, C. Hu, and J. Kouvetakis, Appl. Phys. Lett. **81**, 2992 (2002).
[22] H. J. McSkimin and P. Andreatch, Jr., J. Appl. Phys. **35**, 3312 (1964).
[23] H. J. McSkimin, J. Appl. Phys. **24**, 988 (1953).
[24] Y. A. Burenkov, S. P. Nikanorov, and A. V. Stepanov, Sov. Phys. Solid State **9**, 1467 (1968); **12**, 2428 (1970).
[25] M. H. Kuok, S. C. Ng, Z. L. Rang, and D. J. Lockwood, Phys. Rev. B **62**, 12902 (2000).
[26] A. V. G. Chizmeshya, M. R. Bauer, and J. Kouvetakis, Chem. Mater. **15**, 2511 (2003).
[27] N. W. Ashcroft and N. D. Mermin, *Solid State Physics* (Holt, Rinehart and Winston, New York, 1976).
[28] B. Mamedov, E. Eser, H. Koç, and I. Askerov, Int. J. Thermophys. **30**, 1048 (2009).
[29] P. W. Sparks and C. A. Swenson, Phys. Rev. **163**, 779 (1967).
[30] P. A. Temple and C. E. Hathaway, Phys. Rev. B **7**, 3685 (1973).
[31] B. A. Weinstein and M. Cardona, Phys. Rev. B **7**, 2545 (1973).
[32] O. Madelung, *Semiconductors*, Landolt-Börnstein, New Series Vol. 41, Pt. A (Springer-Verlag, Berlin, New York, 2001).
[33] F. J. Webb and J. Wilks, Proc. R. Soc. London, Ser. A **230**, 549 (1955).
[34] P. Pavone, R. Bauer, K. Karch, O. Sch¸tt, S. Vent, W. Windl, D. Strauch, S. Baroni, and S. de Gironcoli, Physica B **219-220**, 439 (1996).
[35] P. Brüesch, *Phonons: Theory and Experiments I* (Springer-Verlag, Berlin, 1986).
[36] V. R. D'Costa, J. Tolle, C. D. Poweleit, J. Kouvetakis, and J. Menéndez, Phys. Rev. B **76**, 035211 (2007).
[37] H. K. Shin, D. J. Lockwood, and J.-M. Baribeau, Solid State Commun. **114**, 505 (2000).
[38] V. R. D'Costa, J. Tolle, R. Roucka, C. D. Poweleit, J. Kouvetakis, and J. Menéndez, Solid State Commun. **144**, 240 (2007).
[39] W. B. Gauster, J. Appl. Phys. **44**, 1089 (1973).
[40] S. Klotz, J. M. Besson, M. Braden, K. Karch, P. Pavone, D. Strauch, and W. G. Marshall, Phys. Rev. Lett. **79**, 1313 (1997).
[41] K. Gaál-Nagy, M. Schmitt, P. Pavone, and D. Strauch, Comput. Mater. Sci. **22**, 49 (2001).
[42] J. Shen, J. Zi, X. Xie, and P. Jiang, Phys. Rev. B **56**, 12084 (1997).
[43] H. M. Kagaya, Y. Kitani, and T. Soma, Solid State Commun. **58**, 399 (1986).